


RESEARCH

Open Access



# T<sub>1</sub>-Mapping and extracellular volume estimates in pediatric subjects with Duchenne muscular dystrophy and healthy controls at 3T

Nyasha G. Maforo<sup>1,2</sup> , Patrick Magrath<sup>1,3</sup>, Kévin Moulin<sup>6</sup>, Jiaxin Shao<sup>1</sup>, Grace Hyun Kim<sup>1,7</sup>, Ashley Prosper<sup>1</sup>, Pierangelo Renella<sup>1,4</sup>, Holden H. Wu<sup>1,2,3</sup>, Nancy Halnon<sup>5</sup> and Daniel B. Ennis<sup>6\*</sup>

## Abstract

**Background:** Cardiovascular disease is the leading cause of death in patients with Duchenne muscular dystrophy (DMD)—a fatal X-linked genetic disorder. Late gadolinium enhancement (LGE) imaging is the current gold standard for detecting myocardial tissue remodeling, but it is often a late finding. Current research aims to investigate cardiovascular magnetic resonance (CMR) biomarkers, including native (pre-contrast) T<sub>1</sub> and extracellular volume (ECV) to evaluate the early on-set of microstructural remodeling and to grade disease severity. To date, native T<sub>1</sub> measurements in DMD have been reported predominantly at 1.5T. This study uses 3T CMR: (1) to characterize global and regional myocardial pre-contrast T<sub>1</sub> differences between healthy controls and LGE + and LGE− boys with DMD; and (2) to report global and regional myocardial post-contrast T<sub>1</sub> values and myocardial ECV estimates in boys with DMD, and (3) to identify left ventricular (LV) T<sub>1</sub>-mapping biomarkers capable of distinguishing between healthy controls and boys with DMD and detecting LGE status in DMD.

**Methods:** Boys with DMD (N = 28, 13.2 ± 3.1 years) and healthy age-matched boys (N = 20, 13.4 ± 3.1 years) were prospectively enrolled and underwent a 3T CMR exam including standard functional imaging and T<sub>1</sub> mapping using a modified Look-Locker inversion recovery (MOLLI) sequence. Pre-contrast T<sub>1</sub> mapping was performed on all boys, but contrast was administered only to boys with DMD for post-contrast T<sub>1</sub> and ECV mapping. Global and segmental myocardial regions of interest were contoured on mid LV T<sub>1</sub> and ECV maps. ROI measurements were compared for pre-contrast myocardial T<sub>1</sub> between boys with DMD and healthy controls, and for post-contrast myocardial T<sub>1</sub> and ECV between LGE + and LGE− boys with DMD using a Wilcoxon rank-sum test. Results are reported as median and interquartile range (IQR). p-Values < 0.05 were considered significant. Receiver Operating Characteristic analysis was used to evaluate a binomial logistic classifier incorporating T<sub>1</sub> mapping and LV function parameters in the tasks of distinguishing between healthy controls and boys with DMD, and detecting LGE status in DMD. The area under the curve is reported.

**Results:** Boys with DMD had significantly increased global native T<sub>1</sub> [1332 (60) ms vs. 1289 (56) ms; *p* = 0.004] and increased within-slice standard deviation (SD) [100 (57) ms vs. 74 (27) ms; *p* = 0.001] compared to healthy controls. LGE− boys with DMD also demonstrated significantly increased lateral wall native T<sub>1</sub> [1322 (68) ms vs. 1277 (58) ms; *p* = 0.001] compared to healthy controls. LGE + boys with DMD had decreased global myocardial post-contrast T<sub>1</sub> [565 (113) ms vs 635 (126) ms; *p* = 0.04] and increased global myocardial ECV [32 (8) % vs. 28 (4) %; *p* = 0.02] compared to

\*Correspondence: dbe@stanford.edu

<sup>6</sup> Department of Radiology, Stanford University, 1201 Welch Road, Room P264, Stanford, CA 94305-5488, USA

Full list of author information is available at the end of the article



© The Author(s) 2020. **Open Access** This article is licensed under a Creative Commons Attribution 4.0 International License, which permits use, sharing, adaptation, distribution and reproduction in any medium or format, as long as you give appropriate credit to the original author(s) and the source, provide a link to the Creative Commons licence, and indicate if changes were made. The images or other third party material in this article are included in the article's Creative Commons licence, unless indicated otherwise in a credit line to the material. If material is not included in the article's Creative Commons licence and your intended use is not permitted by statutory regulation or exceeds the permitted use, you will need to obtain permission directly from the copyright holder. To view a copy of this licence, visit <http://creativecommons.org/licenses/by/4.0/>. The Creative Commons Public Domain Dedication waiver (<http://creativecommons.org/publicdomain/zero/1.0/>) applies to the data made available in this article, unless otherwise stated in a credit line to the data.

LGE— boys. In all classification tasks,  $T_1$ -mapping biomarkers outperformed a conventional biomarker, LV ejection fraction. ECV was the best performing biomarker in the task of predicting LGE status (AUC = 0.95).

**Conclusions:** Boys with DMD exhibit elevated native  $T_1$  compared to healthy, sex- and age-matched controls, even in the absence of LGE. Post-contrast  $T_1$  and ECV estimates from 3T CMR are also reported here for pediatric patients with DMD for the first time and can distinguish between LGE+ from LGE— boys. In all classification tasks,  $T_1$ -mapping biomarkers outperform a conventional biomarker, LVEF.

**Keywords:** Duchenne muscular dystrophy, Cardiomyopathy, Cardiovascular magnetic resonance, Extracellular volume fraction, Late gadolinium enhancement, Myocardial remodeling,  $T_1$  mapping

## Background

Cardiovascular disease is the leading cause of death in patients with Duchenne muscular dystrophy (DMD) [1–3]—a fatal X-linked genetic disorder characterized by progressive skeletal, respiratory, and cardiac muscle weakness. DMD affects 15.9 to 19.5 per 100,000 live births, making it the most common muscular dystrophy in kids and fatal genetic disorder. Advancements in respiratory clinical management has enabled boys with DMD to live longer, thereby revealing the cardiac complications that arise. DMD is associated with a variable onset of pediatric cardiomyopathy and heart failure by early adulthood [1, 3]. Clinical evidence of cardiac dysfunction is frequently limited to imaging findings until severe or end-stage cardiomyopathic change has occurred since symptom recognition is difficult in non-ambulatory patients. Consequently, sensitive imaging methods are helpful to identify early cardiac involvement in this high-risk population.

Ongoing efforts to develop DMD-specific therapies may prolong life as they delay the onset of cardiomyopathy in this patient population. However, evaluating the cardiovascular response to novel therapies proves challenging due to the lack of validated cardiac imaging biomarkers for DMD disease progression. Echocardiography and cine cardiovascular magnetic resonance (CMR) imaging enables quantitative estimates of global left ventricular (LV) function including systolic and diastolic volumes, myocardial strain, and LV ejection fraction (LVEF). These metrics, however, are only sensitive to overt functional changes and do not provide insight to microstructural remodeling that may contribute to sub-clinical changes in heart health, fomenting myocardial fibrosis, and overall disease progression.

Cardiac microstructural remodeling in DMD has been identified on pathology as progressive fibrofatty infiltration in the sub-epicardium of the LV free wall, most notably at the base of the heart [4, 5]. This level of myocardial remodeling can also be detected using the conventional late gadolinium enhancement (LGE), which is the current gold standard for detecting myocardial tissue remodeling. LGE imaging has utility for detecting focal

replacement fibrosis, but it is often a late finding (mean onset observed at  $15.2 \pm 5.1$  years [6]) and it underestimates the extent of cardiac involvement because it does not quantify the level of diffuse fibrosis. Diffuse fibrosis, however, is an earlier indicator of cardiac involvement in this population [6, 7]. Due to its need for contrast administration, LGE imaging may be considered invasive and make it challenging for pediatric patients to endure. Increasingly, there exists interest in non-contrast CMR methods to evaluate myocardial remodeling. Importantly, a biomarker capable of detecting early myocardial remodeling prior to LGE can significantly improve the care of boys with DMD. This is especially important given the certainty with which boys will develop cardiac involvement, but the uncertainty associated with the timing of the onset.

Emerging CMR biomarkers have shown promise in quantifying myocardial remodeling by  $T_1$ -mapping, whereby tissue-specific changes can be monitored over time in several cardiac pathologies [8]. To date,  $T_1$  mapping studies in DMD have been reported predominantly at 1.5 T and have demonstrated the ability of native (pre-contrast) LV myocardial  $T_1$  measurements to distinguish between healthy hearts and hearts with positive LGE (LGE+) and negative LGE (LGE—) findings in boys with DMD [4, 8–11]. One study revealed shortened LV myocardial post-contrast  $T_1$  as another measure of fibrosis that may be detected prior to LGE+ findings in DMD [11]. Additionally, from pre- and post-contrast  $T_1$  measurements (and if the patient's hematocrit is measured), the extracellular volume (ECV) fraction can be calculated and used to quantify diffuse fibrosis [12].

The clinical use of 3T CMR continues to increase due to the wide installation base and owing to its many advantages: higher signal-to-noise (SNR) and contrast-to-noise ratio (CNR), faster acquisition times, and more effective functional and microstructural imaging [17, 18]. However, no reports are currently available for native  $T_1$  and ECV estimates in pediatric patients with DMD at 3T. Herein we aim to use 3T CMR: (1) to characterize global and regional myocardial native  $T_1$  differences between boys with DMD and healthy controls; (2) to report global

and regional myocardial post-contrast  $T_1$  values and myocardial ECV estimates in boys with DMD; and (3) to identify LV  $T_1$ -mapping biomarkers capable of distinguishing between healthy controls and boys with DMD and detecting LGE status in DMD.

## Methods

### Study enrollment

This two-center prospective CMR study was approved by both Institutional Review Boards and completed between January 2017 and January 2020. We obtained parental consent and child assent for all study participants under the age of 18 years. Boys with DMD were recruited from one of two children's hospitals on a referral basis from two counties with large urban populations. DMD diagnosis was confirmed by genetic testing to identify the presence of a dystrophin mutation. Boys with DMD did not require respiratory support and were not enrolled in any therapeutic clinical trial at the time of the study. Healthy participants were recruited from the surrounding communities and had no history of cardiovascular disease. Site-A enrolled 13 healthy controls and 21 boys with DMD. Site-B enrolled 7 healthy controls and 7 boys with DMD. In total, 28 boys with DMD and 20 sex-matched healthy controls were enrolled. Table 1 displays the demographic information for the two groups and a summary of medications taken by boys with DMD at the time of the CMR exam.

### Cardiovascular magnetic resonance

After providing informed consent, all 45 participants underwent 3 T CMR (Skyra, Siemens Healthineers, Erlangen, Germany) at each site, using identical software, coils, and scan protocol. The CMR exam included standard functional imaging using a high spatial and temporal resolution, free-breathing retrospectively binned balanced steady state free precession (bSSFP) cine sequence [19, 20] with the following acquisition parameters: 40° flip angle, 6/8 partial Fourier and rate-4 parallel imaging, matrix size 192 × 144, pixel size 1.9 mm × 1.9 mm, slice thickness 8 mm, bandwidth (BW) 930 Hz/Px, TE/TR 1.2 ms/2.4 ms echo spacing, and a temporal resolution of 64.4 ms. Breath-held bSSFP cine was used in six study participants when the free-breathing sequence was unavailable. Parameters for this acquisition were: 58° flip angle, rate-3 parallel imaging, matrix size 256 × 192, pixel size 1.6 mm × 1.6 mm, slice thickness 6 mm, BW 977 Hz/Px, TE/TR 1.4 ms/3.3 ms echo spacing, and a temporal resolution of 32.5 ms. All cine imaging spanned the entire LV from base to apex using short-axis slices.

**Table 1 Demographics of healthy controls and boys with DMD**

	Healthy Controls N = 20	DMD N = 28
Age (years)	13 (4.0) range (9–21)	13 (4.5) range (9–21)
Male (%)	100%	100%
Height* (cm)	165 (21)	135 (26)
Weight (kg)	51 (15)	50 (28)
BMI* (kg/m <sup>2</sup> )	18.2 (3.4)	25.5 (10.2)
BSA* (m <sup>2</sup> )	1.5 (0.3)	1.4 (0.4)
Heart rate* (bpm)	69 (30)	84 (24)
Ambulatory (%)	20 (100%)	3 (10.7%)
Ventilatory Support (%)	0%	0%
<i>Race</i>		
Caucasian	15	15
African American	1	1
Asian	2	5
Other	2	5
Mixed	0	2
<i>Ethnicity</i>		
Hispanic/Latino	7	10
<i>Medications at CMR</i>		
ACEi	0	21 (75%)
ARB	0	4 (14%)
$\beta$ -blocker	0	7 (25%)
Corticosteroids	0	18 (64%)
Diuretic	0	16 (57%)

ACEi, Angiotensin Converting Enzyme Inhibitor; ARB, Angiotensin Receptor Blocker; BMI, body mass index; BSA, body surface area

\*  $p \leq 0.05$ ; Results are presented as median (IQR)

Myocardial  $T_1$  measurements were acquired using a modified Look-Locker inversion recovery (MOLLI) sequence with MOtion Correction (MOCO) [11] in a single mid-ventricular short-axis (SAX) slice and was performed with electrocardiographic (ECG)-gating and breath holding. Pre- and post-contrast  $T_1$  mapping was acquired with a 5(3 s)3 and a 4(1 s)3(1 s)2 MOLLI scheme, respectively. Typical native  $T_1$  imaging parameters were: non-selective inversion pulse, bSSFP single shot readout with a 20° excitation flip angle, 7/8 partial Fourier and rate-2 parallel imaging, matrix size 192 × 132, pixel size 1.9 mm × 1.9 mm, slice thickness 8 mm, BW 1085 Hz/Px, minimum inversion time (TI) of 100 ms and incremented by 80 ms, TE/TR 1.01 ms/2.44 ms echo spacing. Typical post-contrast  $T_1$  imaging parameters were: non-selective inversion pulse, bSSFP single shot read out with a 20° excitation flip angle, 7/8 partial Fourier and rate-2 parallel imaging, matrix size 192 × 164, pixel size 1.9 mm × 1.9 mm, slice thickness 8 mm, BW 1085 Hz/Px, minimum TI of 100 ms with 80 ms increments, TE/TR 1.01 ms/2.44 ms echo spacing. For heart

rates greater than 90/min, the matrix size was decreased to  $192 \times 128$  to mitigate any heart rate biases. Two subjects were inadvertently scanned with the 4(1 s)3(1 s)2 MOLLI scheme for their pre-contrast scan. We have found that this error does not significantly impact the group pre-contrast results. We computed the percent error between each such subject's pre-contrast  $T_1$  and the group pre-contrast mean and found the measurements themselves do not vary significantly from the group mean (percent error  $< 5\%$  for both measurements).

Gadobenate dimeglumine contrast (Gd-BOPTA, MultiHance, Bracco Diagnostics, Milan, Italy) was administered either by hand or computer controlled injection only to boys with DMD. Eight minutes following contrast administration, LGE imaging with a free breathing motion corrected phase sensitive inversion recovery (PSIR) sequence [21] was acquired in the short axis (SAx) view spanning base to apex using the following parameters:  $20^\circ$  flip angle, rate-2 parallel imaging, matrix size  $192 \times 120$ , pixel size  $1.4 \text{ mm} \times 1.4 \text{ mm}$ , slice thickness 6 mm, BW 977 Hz/Px, TE/TR 2.01 ms/2.83 ms echo spacing, and a temporal resolution of 35.1 ms. Vertical long axis (VLA) and horizontal long axis (HLA) views were also acquired. Approximately 18 min ( $18 \pm 6.1$  min) after contrast injection, post-contrast  $T_1$  mapping was performed at slice locations matched to the pre-contrast acquisition. The MOCO  $T_1$  (pre- and post-contrast) maps were generated on the scanner and later used for calculating ECV maps. All boys with DMD provided a blood sample on the day of the CMR exam for measurement of hematocrit to be used in calculating the subject specific ECV.

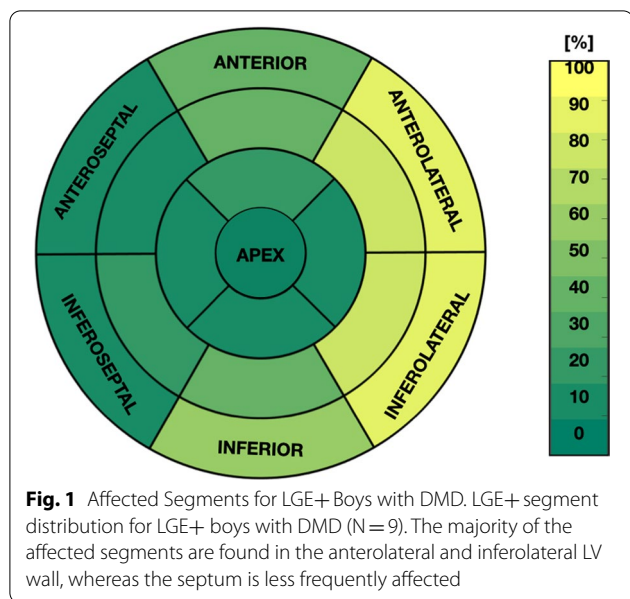
### Post-processing and analysis

Two expert clinicians (either PR or AP) contoured the images, individually at their respective site, using Circle CVI42 (Circle Cardiovascular Imaging Inc., Calgary, Canada) and Medis (Medis Cardiovascular Imaging, Leiden, the Netherlands). They calculated and analyzed the following functional metrics: LV end systolic volume (LVESV) and end diastolic volume (LVEDV), ejection fraction (LVEF), and LV mass (LVM). Parameters were indexed by body surface area (BSA) to derive LVESVI, LVEDVI, and LVMI. A normal LVEF was defined as  $LVEF \geq 55\%$  [22]. Additionally, the clinicians noted the presence or absence of LGE and indicated the number of affected segments according to the American Heart Association (AHA) 17-segment model [23]. A patient with LGE presence in at least one myocardial segment was considered to be LGE positive (LGE+). If no enhancement was observed, then the subject was identified as LGE negative (LGE-). 26 LGE exams were

analyzed by both clinicians with two exams excluded due to poor image quality.

Pre- and post-contrast  $T_1$  maps were registered using a combination of two-dimensional rigid and affine image registration techniques using MATLAB (MathWorks, Natick, Massachusetts, USA) software, then combined with each DMD participant's hematocrit to calculate an ECV map [9]. A region of interest (ROI) encompassing the LV myocardium, and two additional ROIs including a septal and lateral wall segment, were manually selected and analyzed. From each ROI, summary statistics including within-slice standard deviation (SD) were extracted for the global, septal, and lateral LV myocardial regions (Additional file 1: Figure S1). An agreement analysis of the  $T_1$  mapping measurements between the two sites was performed to ensure the applicability of both DMD and healthy control data in the group-wise comparisons. Site-specific measurements were compared using a Wilcoxon-rank sum test.

Demographics for the boys with DMD and healthy controls were compared using a Wilcoxon rank-sum test. Following skewness and kurtosis tests for normality, group-wise comparisons of segmental and global myocardial pre-contrast  $T_1$  were performed with a Wilcoxon rank-sum test between boys with DMD and healthy controls. The segmental and global myocardial post-contrast  $T_1$  and ECV data were compared for two DMD sub-groups (LGE+ vs. LGE-). Furthermore, the within-slice standard deviation (SD) for pre-contrast and post-contrast  $T_1$  and ECV was evaluated in an effort to characterize differences in myocardial tissue heterogeneity between boys with DMD and healthy controls, and also between the two DMD sub-groups. After post hoc correction for multiple comparisons, a  $p$ -Value  $< 0.05$  was considered significant. Due to the varied progression of DMD within this patient cohort and non-normal distribution of the CMR measurements, data is reported as median and interquartile range (IQR). A linear-regression analysis was used to identify initial correlations between  $T_1$  metrics and LV function in boys with DMD and healthy controls.  $R^2$  and  $p$ -Values are reported. Multiple-regression analysis was then used to test for correlations between  $T_1$ -mapping (pre- and post-contrast  $T_1$ , and ECV) measured from lateral wall segments, and global functional metrics (LVEF, LVEDVI, LVESVI, LVMI), and Age, BMI, and heart rate covariates. A binomial logistic regression classifier was analyzed using Receiver Operating Characteristic (ROC) analysis for each measured biomarker in the following distinguishing tasks: (1) healthy controls vs. DMD; (2) healthy controls vs. LGE- boys with DMD; and (3) LGE- vs. LGE+ boys with DMD. Results are displayed by ROC curves and the area under the ROC curve (AUC) is reported. ROC



curves and AUCs are compared for each individual biomarker. A combination (native  $T_1$  and LVEF) is used to evaluate the discriminatory power of non-contrast biomarkers. All statistical analyses were performed in MATLAB (Mathworks).

## Results

### Demographics

We found four significant demographic differences between the two groups: boys with DMD had faster heart rates and were shorter, resulting in larger BMI and smaller BSA values compared to healthy controls (Table 1).

### LV volume and function

Boys with DMD had significantly reduced LVEF [49.5 (11.3) % vs 55.9 (5.8) %];  $p$ -value = 0.003] and lower LVMI [35.6 (9.8) g/m<sup>2</sup> vs 38.4 (7.8) g/m<sup>2</sup>;  $p$ -value = 0.04]. Among boys with DMD, 17 out of the 28 (61%) presented with reduced LVEF. There were no significant

differences in LVEDVI, and LVESVI between the two groups, but boys with DMD had a smaller LVEDVI and larger LVESVI compared to healthy controls. Indices of LV function are displayed in Table 2.

### Late gadolinium enhancement

Nine (32%) of the DMD boys were LGE+ with at least one myocardial segment. Figure 1 shows the distribution of LGE+ segments for all nine LGE+ boys with DMD. Furthermore, all LGE+ boys had enhancement present in the mid-ventricular slice used for  $T_1$  mapping. One significant demographic difference was observed in this group: LGE+ DMD boys had a lower heart rate [73.5 (14.5) bpm vs 96 (28.8) bpm;  $p$ =0.01] compared to LGE- patients. For all LGE+ boys with DMD, the clinicians observed enhancement present at the lateral LV wall, but in two boys, enhancement was also present at the septal wall. LGE+ patients with DMD had a significantly larger LVEDVi [91.8 (39.6) g/m<sup>2</sup> vs. 68.2 (26.8) g/m<sup>2</sup>;  $p$ =0.02] and LVESVI [45.5 (28.7) g/m<sup>2</sup> vs 36.4 (9.7) g/m<sup>2</sup>;  $p$ =0.001] and lower LVEF than LGE- patients with DMD [44.8 (10.7) % vs 55.2 (10.9) %;  $p$ =0.005].

### $T_1$ mapping between sites

We performed an agreement analysis between the two sites (i.e. Site-A and Site-B) and found no statistically significant differences in the measured native  $T_1$  values between healthy controls (Fig. 2a) and boys with DMD (Fig. 2b). Similarly, no significant difference was observed in ECV measurements (Fig. 2d) between the two sites. Post-contrast  $T_1$  measurements between the two sites, however, were found significantly different for all three regions of interest (global, septal, and lateral) as seen in Fig. 2c. Post-contrast measurements from Site-B were significantly lower than measurements from Site-A. To better understand these site specific differences, we further assessed the pre- and post-contrast blood pool  $T_1$  measurements from all controls and

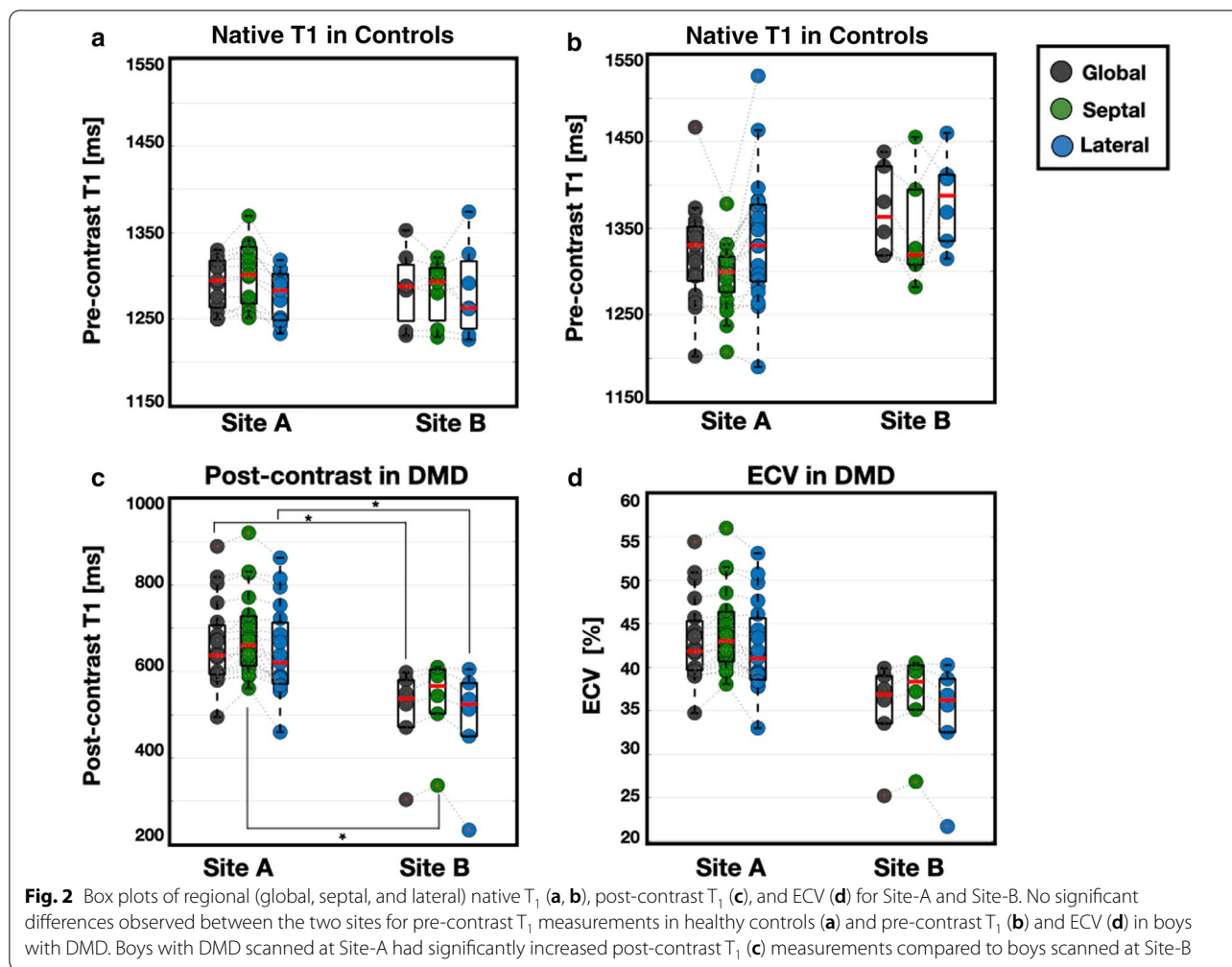
**Table 2** Metrics of left ventricular function from standard CMR

	Healthy Control N = 20	DMD N = 28	$p$ -Value	DMD LGE- N = 17	$p$ -value	DMD LGE+ N = 9	$p$ -Value
LVEF (%)	55.9 (5.8)	49.5 (11.3)	0.003	55.2 (10.9) <sup>#</sup>	0.20	44.8 (10.7)	<0.001
LVEDVI (ml/m <sup>2</sup> )	87.7 (15.2)	82.8 (27.9)	0.10	68.2 (26.8) <sup>#</sup>	0.02	91.8 (39.6)	0.81
LVESVI (ml/m <sup>2</sup> )	38.5 (8.5)	38.7 (14.5)	0.89	36.4 (9.7) <sup>#</sup>	0.02	45.5 (28.7)	0.03
LVMI (g/m <sup>2</sup> )	38.4 (7.8)	35.6 (9.8)	0.04	32.4 (8.4)	0.02	39.5 (8.7)	0.94

All subgroups compared to healthy controls.  $p$ -value  $\leq$  0.05 is significant

LVEF, left ventricular ejection fraction; LVEDVI left ventricular end-diastolic volume; LVESVI left ventricular end-systolic volume; LVMI left ventricular mass index; LGE-, late gadolinium enhancement negative; LGE+, late gadolinium enhancement positive

<sup>#</sup>  $p$   $\leq$  0.05 comparison between LGE- and LGE+ boys



boys with DMD, the blood hematocrit, and the average time after contrast injection for boys with DMD (Table 3). Significant differences were found only in the post-contrast blood pool measurements [406 (197) ms vs. 324 (100) ms;  $p = 0.03$ ] between Site-A and Site-B and in the blood hematocrit measurements [44 (2.4) % vs. 40 (3.0) %;  $p = 0.01$ ], respectively.

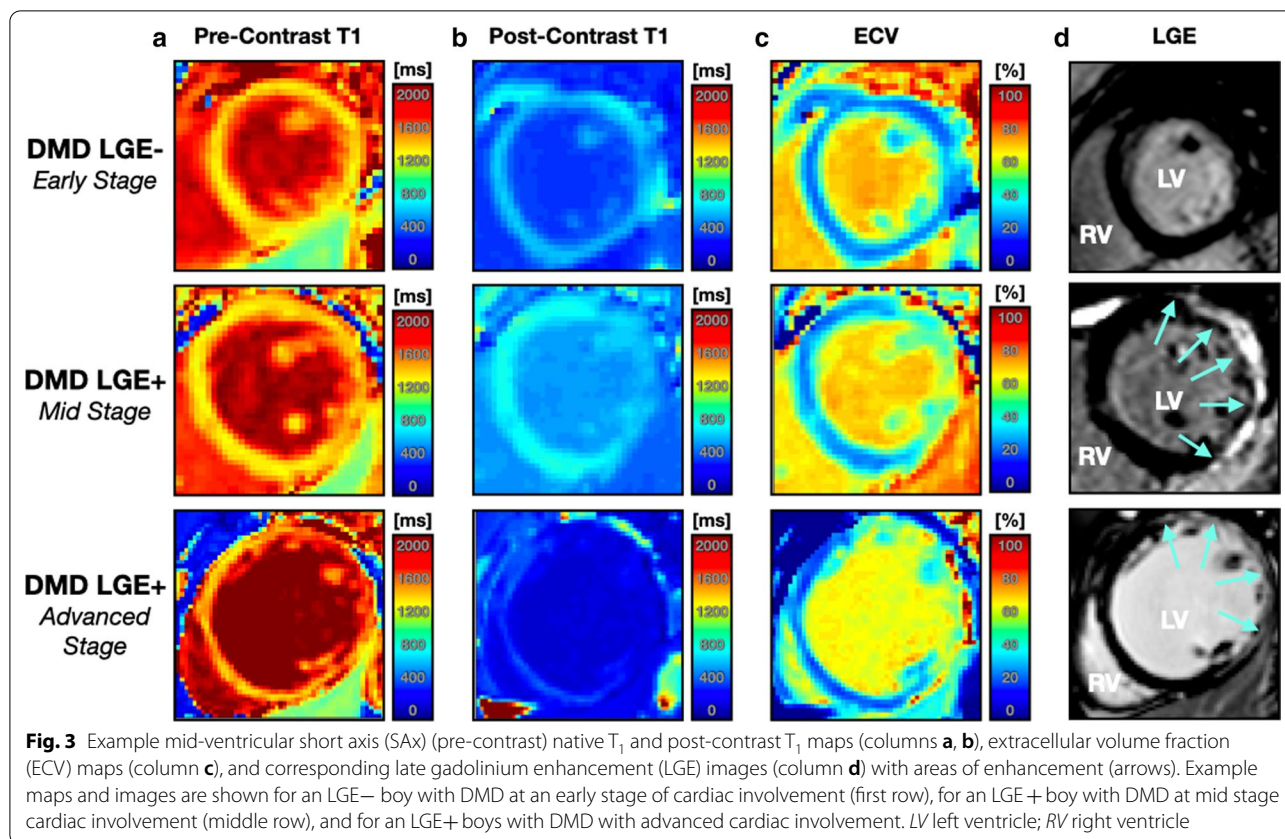
**$T_1$  mapping and extracellular volume in DMD**

All native  $T_1$  maps were analyzed for the healthy controls. Within the DMD cohort, three patients were unable to complete the entire CMR exam resulting in 27 (96%) native  $T_1$ , and 25 (89%) post-contrast  $T_1$  and ECV maps analyzed. Figure 3 displays example pre-contrast and post-contrast  $T_1$  maps (columns A-B), ECV maps (column C), and LGE images (column D) for three boys with DMD at varying stages of cardiac involvement. Guided by previous studies [24, 25], boys

with DMD for this study were defined to be in the early stages of cardiac involvement if they were LGE– with normal LVEF. Mid-stage patients were defined more broadly: (1) either a patient was LGE– with reduced LVEF or; (2) also if the patient was LGE+ with normal LVEF. Advanced stage cardiac involvement was defined

**Table 3 Site-specific  $T_1$  measurements**

Parameter	Site A	Site B	p-Value
Control pre-contrast blood pool $T_1$ (ms)	1881 (62)	1801 (79)	0.10
DMD pre-contrast blood pool $T_1$ (ms)	1816 (137)	1881 (105)	0.10
DMD post-contrast blood pool $T_1$ (ms)	406 (197)	324 (100)	0.03
DMD blood hematocrit (%)	44 (2.4)	40 (3.0)	0.01
Average time after contrast injection (min)	17 (7.9)	18 (9.3)	0.77



as LGE+ with reduced LVEF and visibly dilated LV. Tables 4 and 5 summarize the  $T_1$  mapping results.

Compared to healthy controls, DMD subjects had significantly increased global myocardial native  $T_1$  [1289 (56) ms vs. 1332 (60) ms;  $p=0.004$ ; Fig. 4] and

**Table 4 Summary  $T_1$  mapping and ECV differences between DMD patients and healthy controls**

	Healthy Control N=20	DMD N=28	LGE– N=17	LGE+ N=9
<i>Native/pre-contrast <math>T_1</math>(ms)</i>				
Global	1289 (56)	1332 (60)*	1315 (57) <sup>#</sup>	1350 (53)*
Septal	1300 (55)	1308 (40)	1299 (38)	1318 (54)
Lateral	1277 (58)	1348 (86)*	1322 (68) <sup>#</sup>	1380 (71)*
<i>Post-contrast <math>T_1</math>(ms)</i>				
Global		598 (96)	635 (126) <sup>#</sup>	565 (113) <sup>#</sup>
Septal		639 (112)	643 (113)	591 (125)
Lateral		591 (128)	613 (134) <sup>#</sup>	542 (93) <sup>#</sup>
<i>ECV (%)</i>				
Global		30 (4)	28 (4)	32 (8)
Septal		27 (3)	27 (4)	27 (4)
Lateral		30 (8)	29 (6) <sup>#</sup>	38 (7) <sup>#</sup>

All subgroups compared to healthy controls

\*  $p$ -value  $\leq 0.05$  is significant

<sup>#</sup>  $p$ -value  $\leq 0.05$  comparison between LGE– and LGE+ patients

significantly increased within-slice pre-contrast  $T_1$  SD [74 (27) ms vs.100 (57) ms;  $p=0.001$ ; Table 5]. In the lateral wall, native  $T_1$  [1348 (86) ms vs. 1277 (58) ms vs.;  $p=0.001$ ] and within-slice native  $T_1$  SD [98 (46) ms vs. 67 (27) ms;  $p=0.001$ ; Table 4] remained significantly

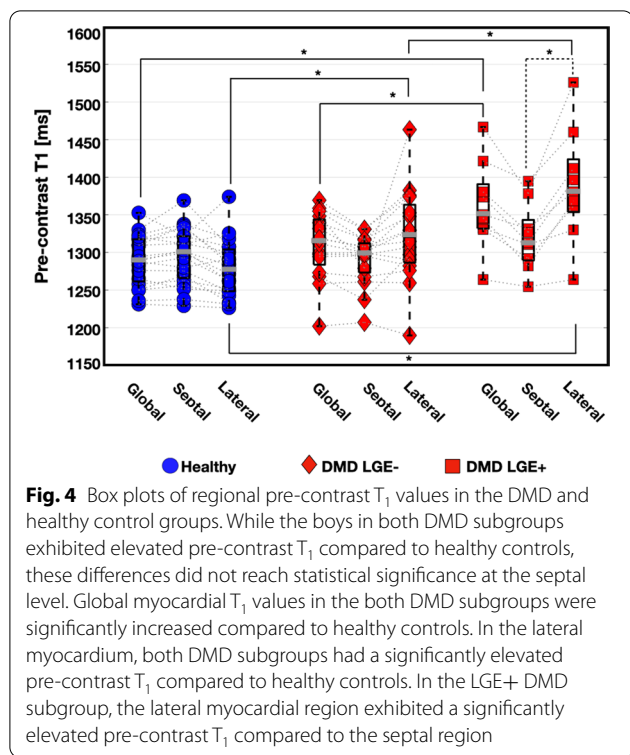
**Table 5 Summary within-slice standard deviation differences between boys with DMD and healthy controls**

	Control N=20	DMD N=28	LGE– N=17	LGE+ N=9
<i>Native/pre-contrast <math>T_1</math> (ms)</i>				
Global	74 (27)	100 (57)*	100 (37)*	104 (61)*
Septal	63 (31)	87 (31)	81 (25)*	92 (46)
Lateral	67 (27)	98 (46)*	91 (29)*	98 (47)*
<i>Post-contrast <math>T_1</math> (ms)</i>				
Global		56 (24)	50 (14) <sup>#</sup>	81 (34)
Septal		39 (18)	35 (12) <sup>#</sup>	52 (14)
Lateral		57 (35)	50 (17) <sup>#</sup>	80 (37)
<i>ECV (%)</i>				
Global		7 (3)	6 (2) <sup>#</sup>	11 (7)
Septal		5 (2)	5 (2)	6 (1)
Lateral		5 (4)	6 (3) <sup>#</sup>	11 (8)

All subgroups compared to healthy controls

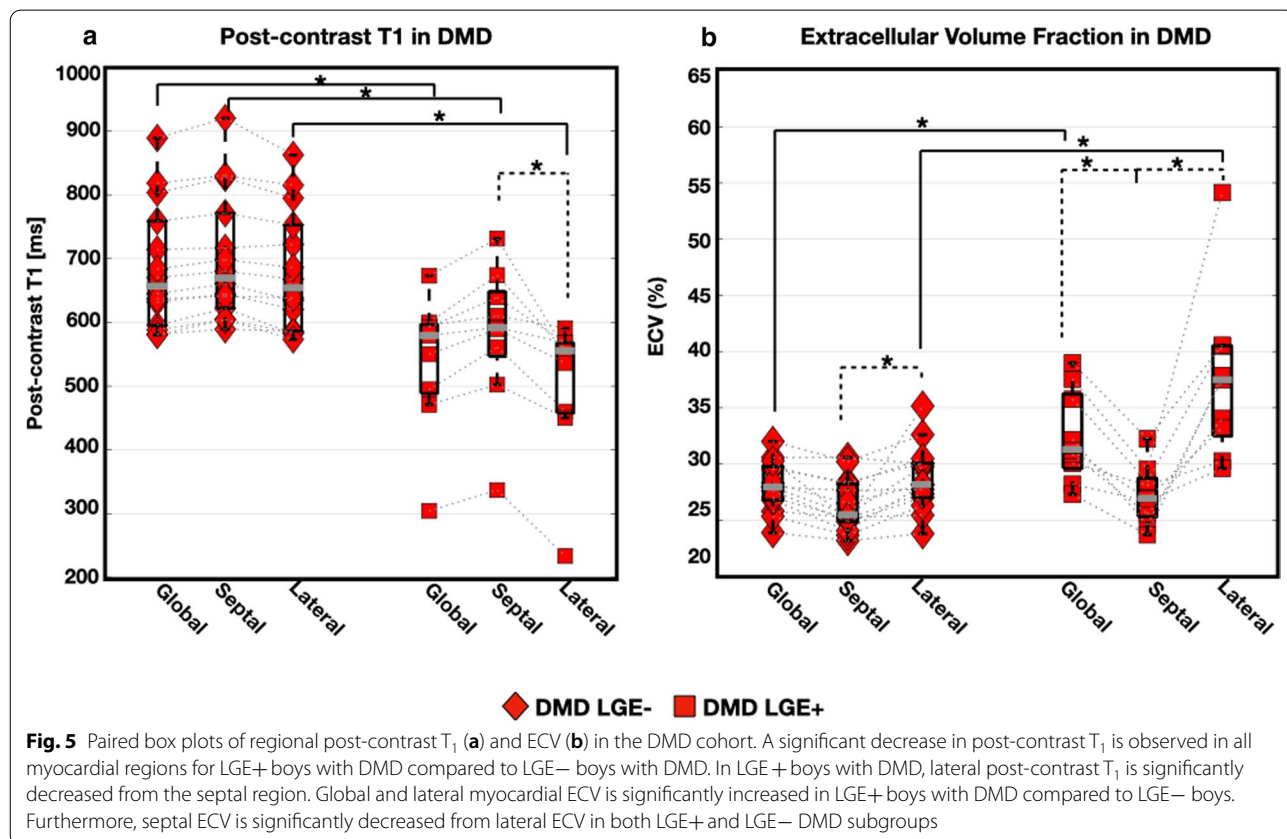
\*  $p$ -value  $\leq 0.05$  is significant

<sup>#</sup>  $p$ -value  $\leq 0.05$  comparison between LGE– and LGE+ patients



increased in boys with DMD compared to healthy controls. The septal myocardium showed no significant differences in native  $T_1$  [1300 (55) ms vs 1299 (38) ms;  $p=0.64$ ; Fig. 4], nor within-slice SD [63 (31) ms vs 87 (31) ms;  $p=0.06$ ; Table 5] between healthy and DMD boys, respectively.

LGE+ boys with DMD had significantly increased native  $T_1$  [1350 (53) ms vs 1315 (57) ms;  $p=0.05$ ] and lateral [1380 (71) ms vs 1322 (68) ms;  $p=0.04$ ] myocardial native  $T_1$  compared to LGE- boys with DMD respectively (Table 4). No significant septal myocardial nor within-slice SD differences were observed between LGE- and LGE+ boys with DMD (Table 5). Lateral myocardial native  $T_1$  was significantly increased in LGE- patients compared to healthy controls [1322 (68) ms vs 1277 (58) ms;  $p=0.02$ ; Fig. 4]. Figure 4 also shows within-group regional  $T_1$  differences for the three groups (controls, LGE+ DMD, and LGE- DMD). Compared to the lateral myocardium, the septal region had significantly lower pre-contrast  $T_1$  values in both DMD subgroups. No significant within-group regional differences were observed in the healthy myocardium. LGE- boys with DMD with normal LVEF were compared against LGE- boys with reduced LVEF, but no significant differences





were observed in native  $T_1$  measurements [1315 (87) ms vs. 1308 (24) ms;  $p=0.93$ ], respectively.

Figure 5 displays regional post-contrast  $T_1$  and ECV measurements from the cohort of boys with DMD. The following septal, and lateral myocardial post-contrast  $T_1$  values were observed: 639 (112) ms, and 591 (128) ms, respectively. A pattern of decreased post-contrast  $T_1$  in the lateral wall compared to measurements in the septal wall was observed, but this difference only reached significance in LGE+ boys with DMD [542 (93) ms vs. 613(134);  $p \leq 0.05$ ]. This pattern of shortened post-contrast  $T_1$  in lateral myocardium is also clearly depicted in Fig. 3.

ECV measurements demonstrated significant differences between the septal and lateral myocardium in patients with DMD [27 (3) % vs. 30 (8) %;  $p=0.001$ ; Fig. 5]. This result is consistent with diffuse fibrosis and extracellular expansion occurring in the DMD disease process [4]. LGE+ boys had a significantly increased lateral myocardial ECV [38 (7) % vs. 29 (6) %,  $p=0.001$ ; Table 4 compared to LGE- boys. However, at the septal level, no significance was reached for ECV [27 (4) % vs. 27 (4) %,  $p=0.73$ ; Table 4] comparison between LGE+ and LGE- boys with DMD. Similar to pre-contrast  $T_1$ , no significant differences were observed in post-contrast  $T_1$  [641 (103) ms vs. 610 (178) ms;  $p=0.49$ ] or ECV [28 (4) % vs. 27 (3) %;  $p=0.57$ ] measurements between LGE- boys with normal LVEF and LGE- boys with reduced LVEF.

#### $T_1$ mapping, extracellular volume, and LV function

Significant correlations between  $T_1$  mapping and metrics of LV function in DMD patients were observed. In the LGE+ group, pre-contrast  $T_1$  and LVEDVI [ $R^2=0.68$ ,  $p=0.01$ ], native  $T_1$  and LVMI [ $R^2=0.56$ ,  $p=0.02$ ], and post-contrast  $T_1$  and LVEF [ $R^2=0.53$ ,  $p=0.03$ ] were significantly correlated. In LGE- boys with DMD, a significant correlation was observed between post-contrast  $T_1$  and LVEF only [ $R^2=0.49$ ,  $p=5.4 \times 10^{-3}$ ]. No  $T_1$  and functional metrics were correlated in healthy controls. Additional file 2: Figure S2 A-D illustrates the significant correlations mentioned above.

The ROC evaluation revealed that a binomial logistic regression classifier using each biomarker in combination with the age, BMI, heart rate, and LVMI as features in all classification tasks resulted in a better model performance than each biomarker alone. Furthermore, the ROC analysis illustrated that all  $T_1$ -mapping biomarkers and LVEF are significant predictors of DMD and LGE status ( $AUC > 0.50$ ); Fig. 6 displays the ROC curves for all the classification tasks. In the task of distinguishing between boys with DMD and healthy controls, native  $T_1$  was comparable to LVEF ( $AUC=0.88$  vs.  $AUC=0.87$ ),

but the combination of pre-contrast  $T_1$  and LVEF yielded the best performance ( $AUC=0.93$ ). Figure 6b displays the same behavior in the LGE- vs. LGE+ boys with DMD using native  $T_1$ , LVEF, and the combination of the two biomarkers ( $AUC=0.84$  vs.  $AUC=0.83$  vs.  $AUC=0.87$ ), respectively. In the task of predicting LGE status, ECV ( $AUC=0.95$ ) outperformed pre- and post-contrast  $T_1$  ( $AUC=0.83$ ,  $AUC=0.93$ ), and LVEF ( $AUC=0.84$ ). The combination of native  $T_1$  and LVEF ( $AUC=0.88$ ) again, performed better in the task of distinguishing between LGE+ vs. LGE- boys with DMD compared to each biomarker performing individually.

#### Discussion

This study used  $T_1$  mapping to define the cardiac micro-structural differences found between pediatric patients with DMD and healthy, sex- and age-matched controls at 3T. To our knowledge, this is the first study to evaluate  $T_1$  mapping in a pediatric DMD study population at 3T. Therefore, these data help to establish reference values for both boys with DMD and healthy controls at 3T. Additionally, the study presented here is the first to investigate a classification model for identifying  $T_1$  mapping differences between boys with DMD and healthy controls and for predicting the presence of pathology associated with LGE status in DMD without requiring contrast. This study further provides evidence to support non-contrast exams in pediatric DMD patients specifically, and can be expanded to investigate  $T_1$  mapping in other cardiomyopathies, particularly in settings when the use of contrast might be contraindicated.

As expected, the 3T native  $T_1$  values reported from this study are elevated relative to previously reported 1.5T pre-contrast  $T_1$  values [6, 14–16, 26]. While elevated, the reported increase in pre-contrast  $T_1$  in boys with DMD compared to healthy controls is consistent with previously published studies at 1.5 T [15, 16, 26]. Taken together these findings further confirm the sensitivity of  $T_1$  mapping for assessing myocardial abnormalities in this population.

Soslow et al. reported increased native  $T_1$  at 1.5T in DMD patients ( $N=31$ ; age  $13.4 \pm 4.7$  years; all males) compared to healthy controls ( $N=11$ ; age  $24.5 \pm 3.9$ ; all males) [1045 ms vs 988 ms,  $p=0.001$ ] [15]. They also demonstrated that this trend remained for LGE- DMD patients with normal LVEF compared to healthy controls. Olivieri et al. demonstrated that DMD boys ( $N=20$ , age  $14.4 \pm 4$  years) also had significantly elevated native  $T_1$  values ( $p < 0.05$ ) compared to healthy sex-matched controls ( $N=16$ ; age  $16.1 \pm 2.2$  years) using both SASHA and MOLLI techniques. Furthermore, when compared to ECV, pre-contrast  $T_1$  demonstrated a 50% increase in the ability to distinguish healthy controls from LGE- boys

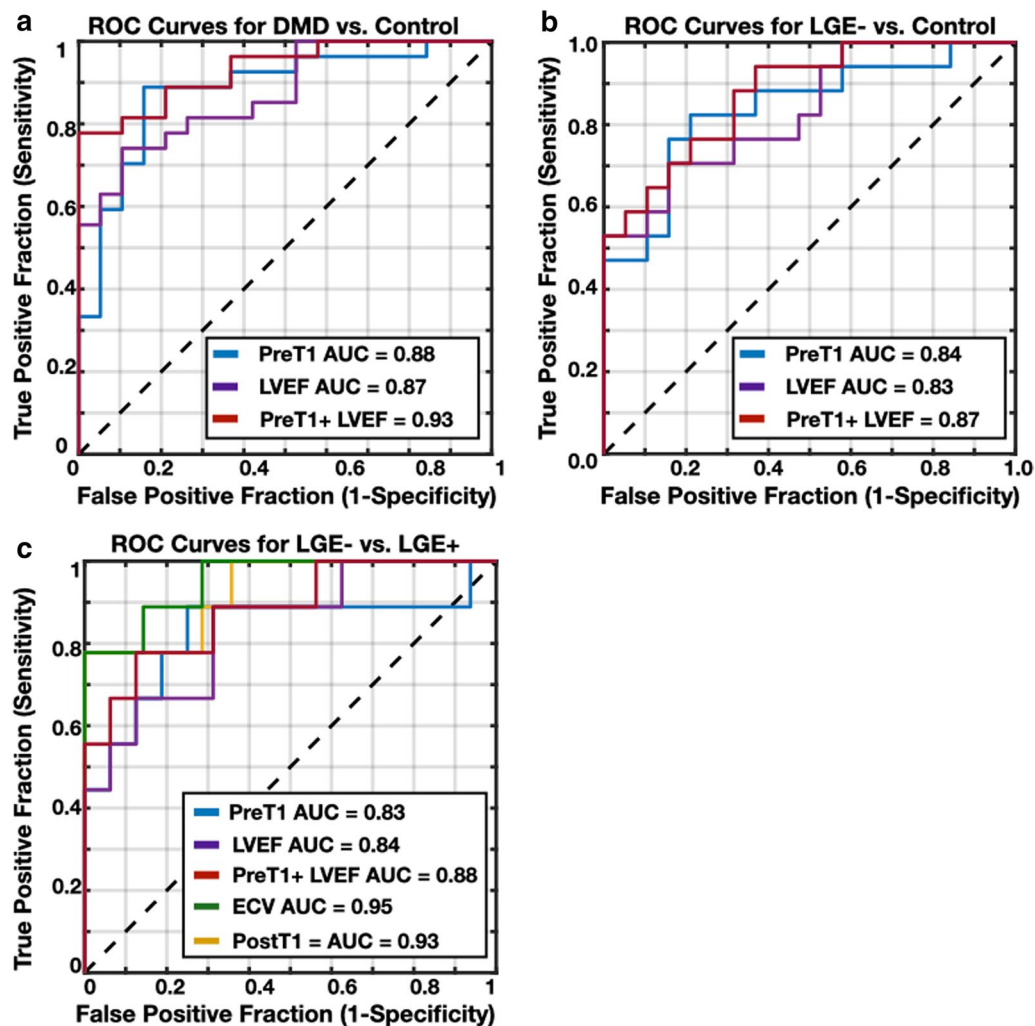


**Fig. 6** Receiver operating characteristic (ROC) curves for individual lateral wall native and post-contrast  $T_1$  mapping biomarker measurements and LVEF from a binomial logistic regression classifier in the task of distinguishing between boys with DMD from healthy controls (a), LGE– boys with DMD from healthy controls (b), and LGE– from LGE+ boys with DMD (c). In all classification tasks,  $T_1$ -mapping biomarkers outperform a conventional biomarker, LVEF. When non-contrast biomarkers (native  $T_1$  and LVEF) are combined, the classification model improves for all three classification tasks, compared to the performance of each biomarker alone. ECV is the best performing biomarker in the task of predicting LGE status

with DMD, and also from LGE+ boys with DMD. Another study at 1.5T by Pavnosky et al. assessed the myocardium of a DMD patient population and also noted a significantly increased native  $T_1$  ( $p < 0.05$ ) in LGE+ and LGE– DMD groups compared to healthy controls.

The native  $T_1$  differences observed in this study (and the above mentioned studies) between DMD patients and healthy controls are consistent with known pathological findings such as fibrosis resulting from extracellular matrix expansion in DMD muscle [6, 9, 27]. Importantly, these changes are detectable even in DMD patients who present with negative findings on LGE exams and therefore provides an earlier indication of

cardiac involvement. The success of using pre-contrast  $T_1$  to detect other pathologies [13] coupled with on-going concerns regarding the use of gadolinium-based contrast agents [28, 29] further motivates the clinical use of pre-contrast  $T_1$ . As shown by the agreement analysis between Site-A and Site-B, pre-contrast  $T_1$  is also more consistent, which makes it better for direct comparisons across sites. Importantly, native  $T_1$  could be used as an early, non-invasive surrogate biomarker for monitoring subclinical cardiac microstructural changes in DMD, thereby enabling earlier and more patient-specific treatment options.

The ECV values reported herein are consistent with previously published pediatric studies [15, 16, 26, 30],

showing the potential for ECV as both a reproducible and repeatable biomarker invariant to magnetic field strength. Furthermore, the global myocardial ECV of DMD patients from this study [ $30 \pm 5\%$ ] was increased compared to that of published healthy controls [ $24 \pm 1\%$  [15]]. Elevated myocardial ECV in DMD subjects compared to healthy controls has been shown by multiple studies [6, 15, 16, 26, 30], thus ECV is promising as a quantitative metric for detecting myocardial microstructural remodeling. Furthermore, this study detected increased ECV in LGE+ patients compared to LGE- patients; a finding also demonstrated by Soslow et al. [15]. The studies by Olivieri et al. [16] and Panovsky et al. [26] only predicted the presence of LGE, but did not distinguish between control subjects and LGE- DMD patients. Such dissimilar findings likely arise due to a variety of cohort specific factors, including the dependence of the results upon the stage of disease.

The regional analysis of pre-contrast and post-contrast  $T_1$  and ECV mapping confirms the disease pattern of fibrosis in the myocardium of boys with DMD. This disease pattern is reported in pathology and imaging studies [27]. Significantly increased native  $T_1$  and ECV, and significantly decreased post-contrast  $T_1$  are observed in the lateral wall compared to septal wall of boys with DMD. These findings are consistent with previously published studies noting that affected myocardial segments predominate in the lateral LV [24, 31–33]. These two myocardial regions experience very different loading conditions, owing to the RV pressure acting on the septum, which may underlie the microstructural differences that arise between these regions [33–35].

The regional abnormalities detected by  $T_1$  mapping are also consistent with the regions in which LGE is present within the DMD myocardium (Fig. 3). While LGE imaging indicates the presence and location of fibrosis,  $T_1$  mapping provides a quantitative description and enables the assessment of myocardial changes that precede the qualitative observance of LGE. In this study, septal  $T_1$  measurements could not distinguish between boys with DMD and healthy controls. Consequently, a regional assessment, as carried out in previous studies [15, 16, 26] provides a more meaningful evaluation of myocardial remodeling in the DMD disease process. In fact, to identify the earliest signs of cardiac involvement in boys with DMD, future studies may focus on more basal slices, wherein cardiac involvement appears earlier.

Furthermore, given the pattern of involvement,  $T_1$  measurements from the septal myocardium may provide a reference (intra-subject control) measure for each individual boy that could provide a way to better monitor microstructural changes over time. Figures 4 and 5 illustrate the regional differences observed in pre-contrast

and post-contrast  $T_1$  and ECV, suggesting that microstructural changes due to DMD predominantly appear in the myocardial lateral wall compared to the septum. In this study, post-contrast  $T_1$  appears to be a weaker determinant of disease stage and severity, as this data only demonstrates significant differences between the septum and lateral myocardium within the LGE+ DMD group. The observation that regional differences are apparent within boys with DMD provides a valuable internal control that mitigates the problems associated with not having post-contrast  $T_1$  values in the control group. These findings further motivate continued use of native  $T_1$  mapping to monitor subclinical changes in the myocardium.

We note significantly greater within-slice standard deviation of native  $T_1$  in boys with DMD compared to healthy controls in both global and regional myocardial measurements, which could provide a biomarker of myocardial tissue heterogeneity. The  $T_1$  values obtained are a complex makeup of signal coming from both cardiomyocyte and extracellular matrix components, thus this finding warrants a  $T_1$  texture analysis to better understand the myocardial tissue differences between boys with DMD and healthy controls.

### Limitations

The study limitations include the general, well-known limitations related to myocardial  $T_1$  mapping [36, 37]. Importantly, significantly faster heart rates were detected in the DMD group compared to the healthy control group. Generally, heart rates are high in DMD and might be related to deconditioning along with changes in cardiac output [38]. As boys with DMD develop advanced cardiomyopathy, angiotensin-converting enzyme inhibitors and beta-blocker therapies are prescribed to lessen the severity of symptoms. This study did not correct for therapy effects on  $T_1$  mapping results. In order to mitigate the heart rate dependencies on  $T_1$  mapping, the sequence parameters used in this study were within recommended guidelines [39, 40].

The CMR data obtained for this study was within known institution-specific ranges and followed very controlled protocols within and between sites. The discrepancy in post-contrast myocardial and blood pool  $T_1$  measurements between Site-A and Site-B maybe described, in part, by the contrast injection method used at each site. At Site-A, contrast was administered via contrast media autoinjector, while hand injection was the method of choice at Site-B. Kinetic measurements of the contrast injection were not acquired, thus it is not currently possible to further assess the individual contrast dynamics and their overall impact on the group-wise

comparisons. This particular sub-analysis is further limited by the group sample sizes.

Recruiting subjects with a rare, complex genetic disease whose cardiac involvement is understudied, is a difficult task—even more so to recruit a well-matched (i.e. age, height, weight) control group. Therefore, this study is limited by its sample size, which further limits subgroup analyses. Herein, the control group did not undergo post-contrast CMR as this would generally be contraindicated and impractical.

## Conclusions

3T CMR native T1 demonstrates the ability to characterize myocardial differences in boys with DMD and healthy, age- and sex-matched controls. Additionally, post-contrast T<sub>1</sub> and ECV estimates in boys with DMD distinguish LGE+ from LGE− myocardium. ROC analysis revealed that in all classification tasks, T<sub>1</sub> mapping biomarkers outperform LVEF, a conventional biomarker. Importantly, both native and post-contrast T<sub>1</sub> and ECV estimates are promising diagnostic CMR biomarkers for assessing myocardial remodeling in Duchenne muscular dystrophy.

## Supplementary information

Supplementary information accompanies this paper at <https://doi.org/10.1186/s12968-020-00687-z>.

**Additional file 1: Figure S1.** Example case from a boy with DMD showing the regions of interest (ROI) manually drawn on a mid-ventricular short-axis (A) pre-contrast/native and (B) post-contrast T1 map and (C) an extracellular volume (ECV) map. (D) The corresponding late gadolinium enhancement (LGE) image with areas of enhancement on the lateral free wall (arrows).

**Additional file 2: Figure S2.** Pre-contrast T1 as a function of LVEDVi (A) and LVMI (B) and Post-contrast T<sub>1</sub> as function of LVEF (C) and LVESVi (D) in healthy controls (gray circles), LGE− (red diamonds) and LGE+ (green squares) boys with DMD. The red solid lines indicate the linear regression fit. Significant correlations are outlined by the dashed-lined rectangles. Significant correlations were observed in the LGE+ group only for the following: 1) native T<sub>1</sub> and LVEDVi; 2) native T1 and LVMI; and 3) post-contrast T<sub>1</sub> and LVEF. In LGE− boys with DMD, a significant correlation was observed between post-contrast T<sub>1</sub> and LVEF only. No T<sub>1</sub> and functional metrics were correlated in healthy controls.

## Abbreviations

AHA: American Heart Association; BMI: Body mass index; BSA: Body surface area; bSSFP: Balanced steady state free precession; CMR: Cardiovascular magnetic resonance; CNR: Contrast-to-noise ratio; DMD: Duchenne muscular dystrophy; ECG: Electrocardiogram; ECV: Extracellular volume fraction; HLA: Horizontal long axis; LGE: Late gadolinium enhancement; LV: Left ventricle/left ventricular; LVEDV: Left ventricular end diastolic volume; LVEDVi: Left ventricular end diastolic volume indexed to BSA; LVEF: Left ventricular ejection fraction; LVESV: Left ventricular end systolic volume; LVESVi: Left ventricular end systolic volume indexed to BSA; LVMI: Left ventricular mass; LVMI: Left ventricular mass indexed to BSA; MOCO: Motion correction; MOLLI: Modified Look-Locker inversion recovery; PSIR: Phase sensitive inversion recover; ROC: Receiver operating characteristic; ROI: Region of interest; Sax: Short axis; SASHA: Saturation recovery single shot acquisition; SNR: Signal-to-noise ratio; T<sub>1</sub>: Longitudinal

relaxation time constant; TE: Echo time; TI: Inversion time; TR: Repetition time; VLA: Vertical long axis.

## Acknowledgements

The authors of this manuscript thank all of the study coordinators and MRI technicians for their help in organizing and executing the studies.

## Authors' contributions

NGM wrote MATLAB software, analyzed CMRs, performed volunteer CMRs, contributed to statistical analysis, and drafted and revised the manuscript. PM contributed to CMR analysis, performed volunteer CMRs, and critically revised manuscript with important intellectual content. KM contributed to the design and testing of the CMR protocol, performed volunteer CMRs, and critically revised the manuscript with important intellectual content. JS contributed to the design and testing of the CMR protocol and revised the manuscript with important intellectual content. GK guided and contributed to the statistical analysis and revised the manuscript with important intellectual content. AP contributed to the analysis of CMRs, revised the manuscript with important intellectual content, and provided DMD specific knowledge and insight. PR contributed to the study design, enrolled patients and healthy controls, analyzed CMRs, provided DMD specific knowledge and insight, and critically revised the manuscript with important intellectual content. HHW provided knowledge and insights relevant to study and critically revised the manuscript with important intellectual content. NH contributed to the study design, enrolled patients and healthy controls, provided DMD specific knowledge and insight, and critically revised the manuscript with important intellectual content. DBE conceived and designed the study, contributed to the analysis, provided knowledge and insights relevant to study, and helped to draft and revise the manuscript with important intellectual content. All authors read and approved the final manuscript.

## Funding

This research was supported by NIH R01 HL131975 to DBE and NSF DGE 1650604 to NGM.

## Availability of data and materials

The datasets used and/or analyzed during the current study are available from the corresponding author on reasonable request.

## Ethics approval and consent to participate

This work was approved by the University of California, Los Angeles Institutional Review Board (IRB). All study participants provided informed consent.

## Consent for publication

Consent for publication was obtained in the institutional consent form approved by the IRB.

## Competing interests

The authors declare that they have no competing interests.

## Author details

<sup>1</sup> Department of Radiological Sciences, University of California, Los Angeles, CA, USA. <sup>2</sup> Physics and Biology in Medicine Interdepartmental Program, University of California, Los Angeles, CA, USA. <sup>3</sup> Department of Bioengineering, University of California, Los Angeles, CA, USA. <sup>4</sup> Department of Medicine, Division of Pediatric Cardiology, CHOC Children's Hospital, Orange, CA, USA. <sup>5</sup> Department of Pediatrics (Cardiology), University of California, Los Angeles, CA, USA. <sup>6</sup> Department of Radiology, Stanford University, 1201 Welch Road, Room P264, Stanford, CA 94305-5488, USA. <sup>7</sup> Department of Biostatistics, University of California, Los Angeles, CA, USA.

Received: 5 February 2020 Accepted: 29 October 2020

Published online: 10 December 2020

## References

1. D'Amario D, Amodeo A, Adorasio R, Tiziano FD, Leone AM, Perri G, et al. A current approach to heart failure in Duchenne muscular dystrophy. *Heart*. 2017;103(22):1770.

2. Van Ruiten HJA, Marini Bettolo C, Cheetham T, Eagle M, Lochmuller H, Straub V, et al. Why are some patients with Duchenne muscular dystrophy dying young: an analysis of causes of death in North East England. *Eur J Paediatr Neurol*. 2016;20(6):904–9.
3. Ryder S, Leadley RM, Armstrong N, Westwood M, de Kock S, Butt T, et al. The burden, epidemiology, costs and treatment for Duchenne muscular dystrophy: an evidence review. *Orphanet J Rare Dis*. 2017;12:79.
4. Frankel KA, Rosser RJ. The pathology of the heart in progressive muscular dystrophy: epimycardial fibrosis. *Hum Pathol*. 1976;7(4):375–86.
5. Azevedo PS, Polegato BF, Minicucci MF, Paiva SAR, Zornoff LAM. Cardiac remodeling: concepts, clinical impact, pathophysiological mechanisms and pharmacologic treatment. *Arq Bras Cardiol*. 2016;106(1):62–9.
6. Florian A, Ludwig A, Rosch S, Yildiz H, Sechtem U, Yilmaz A. Myocardial fibrosis imaging based on T1-mapping and extracellular volume fraction (ECV) measurement in muscular dystrophy patients: diagnostic value compared with conventional late gadolinium enhancement (LGE) imaging. *Eur Heart J Cardiovasc Imaging*. 2014;15(9):1004–12.
7. Mavrogeni S, Papavasiliou A, Giannakopoulou K, Markousis-Mavrogenis G, Pons MR, Karanasios E, et al. Oedema-fibrosis in Duchenne muscular dystrophy: role of cardiovascular magnetic resonance imaging. *Eur J Clin Invest*. 2017. <https://doi.org/10.1111/eci.12843>.
8. Everett RJ, Stirrat CG, Semple SIR, Newby DE, Dweck MR, Mirsadraee S. Assessment of myocardial fibrosis with T1 mapping MRI. *Clin Radiol*. 2016;71(8):768–78.
9. Jerosch-Herold M, Kwong RY. Cardiac T1 Imaging. *Top Magn Reson Imaging*. 2014;23(1):3–11.
10. Puntmann VO, Voigt T, Chen Z, Mayr M, Karim R, Rhode K, et al. Native T1 mapping in differentiation of normal myocardium from diffuse disease in hypertrophic and dilated cardiomyopathy. *JACC Cardiovasc Imaging*. 2013. <https://doi.org/10.1016/j.jcmg.2012.08.019>.
11. Messroghli DR, Radjenovic A, Kozerke S, Higgins DM, Sivananthan MU, Ridgway JP. Modified Look-Locker inversion recovery (MOLLI) for high-resolution T1 mapping of the heart. *Magn Reson Med*. 2004. <https://doi.org/10.1002/mrm.20110>.
12. Chow K, Flewitt JA, Green JD, Pagano JJ, Friedrich MG, Thompson RB. Saturation recovery single-shot acquisition (SASHA) for myocardial T1 mapping. *Magn Reson Med*. 2014;71(6):2082–95.
13. Dass S, Suttie JJ, Piechnik SK, Ferreira VM, Holloway CJ, Banerjee R, et al. Myocardial tissue characterization using magnetic resonance non-contrast t1 mapping in hypertrophic and dilated cardiomyopathy. *Circ Cardiovasc Imaging*. 2012. <https://doi.org/10.1161/CIRCIMAGING.112.976738>.
14. Soslow JH, Damon BM, Saville BR, Lu Z, Burnette WB, Lawson MA, et al. Evaluation of post-contrast myocardial t1 in duchenne muscular dystrophy using cardiac magnetic resonance imaging. *Pediatr Cardiol*. 2015;36(1):49–56.
15. Soslow JH, Damon SM, Crum K, Lawson MA, Slaughter JC, Xu M, et al. Increased myocardial native T1 and extracellular volume in patients with Duchenne muscular dystrophy. *J Cardiovasc Magn Reson*. 2016;18:5.
16. Olivieri LJ, Kellman P, McCarter RJ, Cross RR, Hansen MS, Spurney CF. Native T1 values identify myocardial changes and stratify disease severity in patients with Duchenne muscular dystrophy. *J Cardiovasc Magn Reson*. 2016;18:72.
17. Rajiah P, Bolen MA. Cardiovascular MR imaging at 3 T: opportunities, challenges, and solutions. *RadioGraphics*. 2014;34(6):1612–35.
18. Saeed M, Van TA, Krug R, Hetts SW, Wilson MW. Cardiac MR imaging: current status and future direction. *Cardiovasc Diagn Ther*. 2015;5(4):290–310.
19. Kellman P, Ched'hotel C, Lorenz CH, Mancini C, Arai AE, McVeigh ER. High spatial and temporal resolution cardiac cine MRI from retrospective reconstruction of data acquired in real time using motion correction and resorting. *Magn Reson Med*. 2009;62(6):1557–64.
20. Xue H, Kellman P, Larocca G, Arai AE, Hansen MS. High spatial and temporal resolution retrospective cine cardiovascular magnetic resonance from shortened free breathing real-time acquisitions. *J Cardiovasc Magn Reson*. 2013;15(1):102–102.
21. Kellman P, Larson AC, Hsu L-Y, Chung Y-C, Simonetti OP, McVeigh ER, et al. Motion-corrected free-breathing delayed enhancement imaging of myocardial infarction. *Magn Reson Med*. 2005;53(1):194–200.
22. Pfeffer MA, Shah AM, Borlaug BA. Heart failure with preserved ejection fraction in perspective. *Circ Res*. 2019;124(11):1598–617.
23. Cerqueira Manuel D, Weissman Neil J, Dilsizian V, Jacobs Alice K, Kaul S, et al. Standardized myocardial segmentation and nomenclature for tomographic imaging of the heart. *Circulation*. 2002;105(4):539–42.
24. Fayssoil A, Abasse S, Silverston K. Cardiac involvement classification and therapeutic management in patients with Duchenne muscular dystrophy. *J Neuromuscul Dis*. 2017;4(1):17–23.
25. Palladino A, D'Ambrosio P, Papa AA, Pettilo R, Orsini C, Scutifero M, et al. Management of cardiac involvement in muscular dystrophies: paediatric versus adult forms. *Acta Myol*. 2016;35(3):128–34.
26. Panovský R, Pešl M, Holeček T, Máchal J, Feitová V, Mrázová L, et al. Cardiac profile of the Czech population of Duchenne muscular dystrophy patients: a cardiovascular magnetic resonance study with T1 mapping. *Orphanet J Rare Dis*. 2019;14(1):10–10.
27. Diao K, Yang Z, Xu H, Liu X, Zhang Q, Shi K, et al. Histologic validation of myocardial fibrosis measured by T1 mapping: a systematic review and meta-analysis. *J Cardiovasc Magn Reson*. 2016;18(1):92.
28. Bhargava R, Hahn G, Hirsch W, Kim M-J, Mentzel H-J, Olsen OE, et al. Contrast-enhanced magnetic resonance imaging in pediatric patients: review and recommendations for current practice. *Magn Reson Insights*. 2013;6:95–111.
29. Lang SM, Alsaied T, Moore RA, Rattan M, Ryan TD, Taylor MD. Conservative gadolinium administration to patients with Duchenne muscular dystrophy: decreasing exposure, cost, and time, without change in medical management. *Int J Cardiovasc Imaging*. 2019. <https://doi.org/10.1007/s10554-019-01670-1>.
30. Starc JJ, Moore RA, Rattan MS, Villa CR, Gao Z, Mazur W, et al. Elevated myocardial extracellular volume fraction in Duchenne muscular dystrophy. *Pediatr Cardiol*. 2017;38(7):1485–92.
31. Ashwath ML, Jacobs IB, Crowe CA, Ashwath RC, Super DM, Bahler RC. Left ventricular dysfunction in duchenne muscular dystrophy and genotype. *Am J Cardiol*. 2014;114(2):284–9.
32. Kamdar F, Garry DJ. Dystrophin-deficient cardiomyopathy. *J Am Coll Cardiol*. 2016;67(21):2533–46.
33. Kvasnicka J, Vokrouhlicky L. Heterogeneity of the myocardium. Function of the left and right ventricle under normal and pathological conditions. *Physiol Res*. 1991;40(1):31–7.
34. Kohl P. Cardiac cellular heterogeneity and remodelling. *Cardiovasc Res*. 2004;64(2):195–7.
35. Solovyova O, Katsnelson LB, Kohl P, Panfilov AV, Tsurian AK, Tsyvian PB. Mechano-electric heterogeneity of the myocardium as a paradigm of its function. *Prog Biophys Mol Biol*. 2016;120(1–3):249–54.
36. McNally EM, Kaltman JR, Benson DW, Canter CE, Cripe LH, Duan D, et al. Contemporary cardiac issues in Duchenne muscular dystrophy. Working Group of the National Heart, Lung, and Blood Institute in collaboration with Parent Project Muscular Dystrophy. *Circulation*. 2015;131(18):1590–8.
37. von Knobelsdorff-Brenkenhoff F, Prothmann M, Dieringer MA, Wassmuth R, Greiser A, Schwenke C, et al. Myocardial T1 and T2 mapping at 3 T: reference values, influencing factors and implications. *J Cardiovasc Magn Reson*. 2013;15(1):53–53.
38. Thomas TO, Morgan TM, Burnette WB, Markham LW. Correlation of heart rate and cardiac dysfunction in Duchenne muscular dystrophy. *Pediatr Cardiol*. 2012;33(7):1175–9.
39. Kellman P, Hansen MS. T1-mapping in the heart: accuracy and precision. *J Cardiovasc Magn Reson*. 2014. <https://doi.org/10.1186/1532-429X-16-2>.
40. Messroghli DR, Moon JC, Ferreira VM, Grosse-Wortmann L, He T, Kellman P, et al. Clinical recommendations for cardiovascular magnetic resonance mapping of T1, T2, T2\* and extracellular volume: a consensus statement by the Society for Cardiovascular Magnetic Resonance (SCMR) endorsed by the European Association for Cardiovascular Imaging (EACVI). *J Cardiovasc Magn Reson*. 2017;19(1):75.

## Publisher's Note

Springer Nature remains neutral with regard to jurisdictional claims in published maps and institutional affiliations.